



Cite this: *Chem. Commun.*, 2015, 51, 9547

Received 23rd February 2015,  
Accepted 24th April 2015

DOI: 10.1039/c5cc01597a

www.rsc.org/chemcomm

# Anion-induced Ag<sup>I</sup> self-assemblies with electron deficient aromatic ligands: anion- $\pi$ -system interactions as a driving force for templated coordination networks†

Damir A. Safin,<sup>a</sup> Amélie Pialat,<sup>a</sup> Alicea A. Leitch,<sup>a</sup> Nikolay A. Tumanov,<sup>b</sup> Iliia Korobkov,<sup>a</sup> Yaroslav Filinchuk,<sup>b</sup> Jaclyn L. Brusso<sup>a</sup> and Muralee Murugesu<sup>\*a</sup>

**Three novel 1D, 2D and 3D coordination polymers were successfully isolated using nitrogen based 3,6-bis(2'-pyrimidyl)-1,2,4,5-tetrazine (BPymTz) and 2,4,6-tris(2-pyrimidyl)-1,3,5-triazine (TPymT) ligands with Ag<sup>I</sup> ions. The formation of these supramolecular assemblies was templated through anion- $\pi$ -system interactions.**

In the last decade, a new type of non-covalent force, commonly referred to as an anion- $\pi$ -system interaction, has received significant interest due to its fundamental role in biological and chemical applications.<sup>1</sup> While the electron donating nature of anions would typically result in repulsion with aromatic  $\pi$ -systems, in this instance that is not the case as the electron deficiency of the aromatic system enables these interactions. Furthermore, the interactions between electron deficient aromatic systems and anions have been shown to be energetically favourable ( $\sim 20$ – $70$  kJ mol<sup>-1</sup>) based on theoretical studies.<sup>2</sup> Consequently, harnessing these interactions can facilitate the creation of coordination networks where the nature of the anions (*e.g.*, size, shape, charge) can be utilized as a driving force for structure formation. While this approach has been successfully employed for the self-assembly of molecular aggregates,<sup>3</sup> it is rarely used in the synthesis of highly dimensional non-discrete structures.<sup>3b</sup>

Recently, it was reported that *s*-triazine and 1,2,4,5-tetrazine rings are efficient receptors for interaction with a variety of anions. In particular, the nature of the anions (PF<sub>6</sub><sup>-</sup>, BF<sub>4</sub><sup>-</sup>, ClO<sub>4</sub><sup>-</sup>) in the corresponding Ag<sup>I</sup> salts controls the self-assembly of the metal cation with 2,4,6-tris(2-pyrimidyl)-1,3,5-triazine.<sup>4</sup> In other studies involving first-row transition metals (Ni<sup>II</sup>, Zn<sup>II</sup>, Mn<sup>II</sup>, Fe<sup>II</sup>, Cu<sup>II</sup>) with 3,6-bis(2-pyridyl)-1,2,4,5-tetrazine or 3,6-bis(2'-pyrimidyl)-1,2,4,5-tetrazine (BPymTz), the anions chosen (SbF<sub>6</sub><sup>-</sup>, PF<sub>6</sub><sup>-</sup>,

BF<sub>4</sub><sup>-</sup>, ClO<sub>4</sub><sup>-</sup>, Br<sub>3</sub><sup>-</sup>, I<sup>-</sup>) played a crucial role in the supramolecular aggregate formation.<sup>3f,5</sup> With this in mind, we intend to exploit anion- $\pi$ -system interactions towards the development of highly ordered supramolecular structures. To that end, BPymTz<sup>6</sup> and 2,4,6-tris(2-pyrimidyl)-1,3,5-triazine (TPymT)<sup>7</sup> are attractive candidates for such interactions as they not only contain  $\pi$ -acidic aromatic moieties (*viz.* *s*-triazine and 1,2,4,5-tetrazine), but also possess coordination environments similar to 2,2'-bipyridine and terpyridine (Chart 1).<sup>1b-f,5,8</sup> Another remarkable feature of these rigid ligands is that they possess multiple chelating pockets on either side, promoting multidimensional growth rather than discrete molecules.

Using this strategy, we herein report the self-assembly of a supramolecular anion-templated (*e.g.*, PF<sub>6</sub><sup>-</sup> and OTf<sup>-</sup>) ribbon-like 1D chain, {[Ag<sub>2</sub>(BPymTz)<sub>2</sub>](PF<sub>6</sub>)<sub>2</sub>·2CH<sub>3</sub>CN}<sub>n</sub> (1), and a honeycomb-like 2D network, {[Ag<sub>4</sub>(BPymTz)<sub>3</sub>](OTf)<sub>2</sub>(CH<sub>3</sub>CN)<sub>2</sub>·2(OTf)·CH<sub>3</sub>CN}<sub>n</sub> (2), based on BPymTz and Ag<sup>I</sup> ions. In addition, we also report the first self-assembled TPymT-based 3D framework, {[AgTPymT](ClO<sub>4</sub>)<sub>n</sub>} (3), with an unprecedented 2-fold interpenetrating coordination network. In all of the presented complexes, the anion- $\pi$ -system interactions between PF<sub>6</sub><sup>-</sup>, OTf<sup>-</sup>, ClO<sub>4</sub><sup>-</sup> and the electron deficient aromatic ligands play a crucial role in the self-assembly of the superstructures (Chart 2).

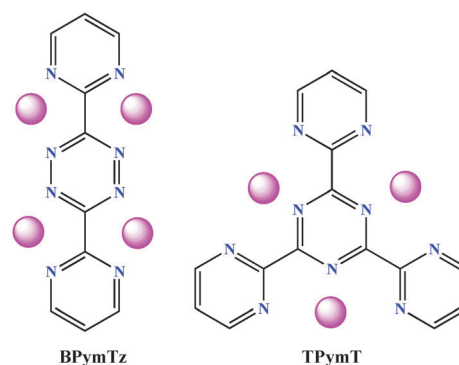


**Chart 1** Ligands employed for the isolation of coordination networks in this study. Pink balls highlight multi-metal coordination sites.

<sup>a</sup> Department of Chemistry, University of Ottawa, 10 Marie Curie Private, Ottawa, ON, Canada K1N 6N5. E-mail: m.murugesu@uottawa.ca; Fax: +1 (613) 562 5170; Tel: +1 (613) 562 5800 ext. 2733

<sup>b</sup> Institute of Condensed Matter and Nanosciences, Université catholique de Louvain, Place L. Pasteur 1, 1348 Louvain-la-Neuve, Belgium

† Electronic supplementary information (ESI) available: Additional data and Fig. S1–S8. CCDC 1028560, 1028561 and 1027767. For ESI and crystallographic data in CIF or other electronic format see DOI: 10.1039/c5cc01597a

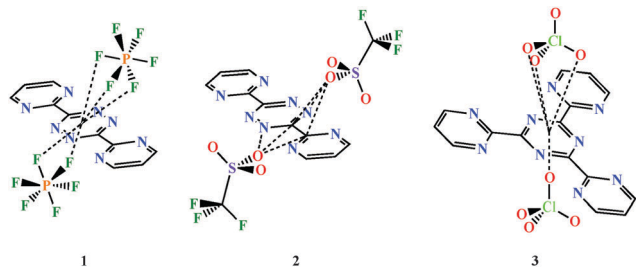


Chart 2 Anion- $\pi$ -system interactions exhibited by **1**–**3**.

The reaction of BPymTz with one equivalent of  $\text{AgPF}_6$  or  $\text{AgOTf}$  in  $\text{CH}_3\text{CN}$  affords purple crystals of **1** or dark grey crystals of **2**, respectively (Fig. S1 and S2, and for details see the ESI<sup>†</sup>). The reaction of TPymT with three equivalents of  $\text{AgClO}_4$  in hot  $\text{H}_2\text{O}$  affords **3** as orange block-like crystals (Fig. S3 and for details see the ESI<sup>†</sup>). The FTIR spectra of **1**–**3** exhibit a strong band of the  $\text{PF}_6^-$ ,  $\text{OTf}^-$  or  $\text{ClO}_4^-$  anions at 835, 1245 and 1082  $\text{cm}^{-1}$ , respectively, together with all the characteristic bands of the parent ligands BPymTz and TPymT.<sup>6,9</sup>

Compounds **1** and **2** crystallize in the orthorhombic  $Pnma$  and monoclinic  $P2_1/n$  space groups, respectively. The asymmetric unit of **1** consists of one  $\text{Ag}^+$  ion, two halves of BPymTz, two  $\text{PF}_6^-$  anions, and one molecule of  $\text{CH}_3\text{CN}$ . The asymmetric unit of **2** contains four  $\text{Ag}^+$  ions, three molecules of BPymTz, four  $\text{OTf}^-$  anions, and three molecules of  $\text{CH}_3\text{CN}$ . In both complexes, each  $\text{Ag}^+$  is coordinated to three ligands *via* the “bipy” coordination pockets of BPymTz affording a distorted trigonal prismatic environment (Fig. 1), while each BPymTz is coordinated to four  $\text{Ag}^+$  ions, thus

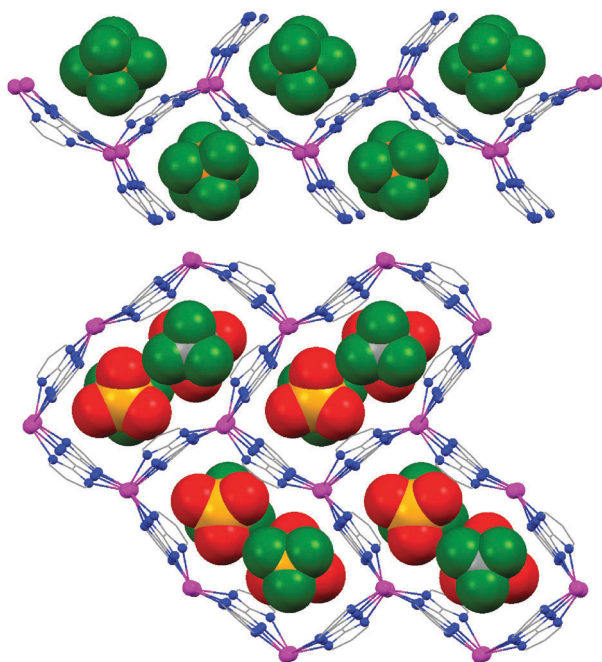


Fig. 1 Ball and stick, and spacefill molecular structures of **1** (top) and the cationic honeycomb-like layers (bottom) in the structure of **2** (hydrogen atoms and disorders were omitted for clarity). Color code: C = grey, F = green, N = blue, Ag = magenta, O = red, S = orange.

promoting the formation of the extended networks. Furthermore, the  $\text{Ag}^+ \cdots \text{Ag}^+$  distances along and across each BPymTz range from 4.25 to 4.28 Å and 6.37 to 6.51 Å for **1** and **2**, respectively. The  $\text{Ag}$ –N(tetrazine) bond distances are within the range of 2.41–2.61 Å, while the  $\text{Ag}$ –N(pyrimidine) bond lengths are slightly shorter (*i.e.*, 2.35–2.50 Å). In both structures the N(tetrazine)– $\text{Ag}$ –N(pyrimidine) angles are  $\sim 65^\circ$  and the BPymTz ligands are essentially planar, with a slight torsion angle between the tetrazine and pyrimidine rings ( $< 12^\circ$ ).

The structure of **1** can be described as a 1D cationic *zig-zag* ribbon running parallel to the  $a$  axis (Fig. 1), which consists of multiple pairs of  $\text{Ag}^+$  ions held together *via* bridging of the BPymTz ligands. Each pair has an additional terminal ligand facing away from either side of the ribbon. The space between the two ribbons is filled with  $\text{PF}_6^-$  anions and  $\text{CH}_3\text{CN}$  molecules. The structure is further stabilized by  $\text{PF}_6^-$ – $\pi$ -system interactions (Chart 2) and C–H $\cdots$ F hydrogen bonds with  $\text{CH}_3\text{CN}$ , which occur between adjacent 1D chains. The closest  $\text{Ag}^+ \cdots \text{Ag}^+$  distance between the two ribbons is 7.34 Å. Each  $\text{PF}_6^-$  anion interacts with the centroids of the tetrazine moiety of the ligand, affording the  $\pi$ -anion linkage with the distances ranging between 2.93 and 3.22 Å.<sup>3h,10</sup> This templating effect of the  $\text{PF}_6^-$  anion drives the overall formation of the extended 1D ribbon-like superstructure.

The structure of **2** can be described as 2D distorted honeycomb-like layers running parallel to the  $a$  axis (Fig. 1). This transformation from a 1D (**1**) to a 2D (**2**) system is driven by the change in the counter anion from  $\text{PF}_6^-$  to  $\text{OTf}^-$  and confirms that anion- $\pi$ -system interactions play a key role in the resulting supramolecular self-assembly. In **2**, each distorted honeycomb-like motif is constructed from six BPymTz ligands linking twelve  $\text{Ag}^+$  ions (Fig. 1). The honeycomb-like cavities contain two  $\text{OTf}^-$  anions and two  $\text{CH}_3\text{CN}$  molecules with the remaining  $\text{OTf}^-$  anions and  $\text{CH}_3\text{CN}$  molecules situated between adjacent 2D layers. The  $\text{OTf}^-$  anions within a honeycomb-like cavity interact with three tetrazine rings with the distances between the oxygen atoms of  $\text{OTf}^-$  and the centroids of the tetrazine rings ranging from 2.93 to 3.68 Å.<sup>10</sup> The  $\text{CH}_3\text{CN}$  molecules inside the cavity exhibit C–H $\cdots$ O and C–H $\cdots$ F contacts with the  $\text{OTf}^-$  anions. The neighbouring honeycomb-like layers are interlinked through the C–H $\cdots$ O and C–H $\cdots$ F interactions. The closest  $\text{Ag}^+ \cdots \text{Ag}^+$  distance between two honeycomb-like 2D layers is 12.27 Å.

In order to determine if the oligomeric structures also exist in solution, electrospray mass spectra (ES MS) studies were performed on  $\text{CH}_3\text{CN}$  solutions of **1** and **2** prior to crystallization. The spectra exhibit a number of peaks due to the formation of different species during the ionization process. For **1**, several oligomers of silver ions BPymTz and  $\text{PF}_6^-$  were detected, which exhibited the expected isotopomer distributions  $[\text{Ag}_2(\text{BPymTz})_2(\text{PF}_6)]^+ m/z$  836.8,  $[\text{Ag}_3(\text{BPymTz})_3(\text{PF}_6)_2]^+ m/z$  1328.7 and  $[\text{Ag}_4(\text{BPymTz})_4(\text{PF}_6)_3]^+ m/z$  1582.5 (Fig. S4, for details see the ESI<sup>†</sup>). Similar observations were made for complex **2**, with the detection of the oligomers  $[\text{Ag}_2(\text{BPymTz})(\text{OTf})]^+ m/z$  602.7,  $[\text{Ag}_3(\text{BPymTz})_2(\text{OTf})_2]^+ m/z$  1098.5 and  $[\text{Ag}_4(\text{BPymTz})_3(\text{OTf})_3]^+ m/z$  1354.3 (Fig. S5, and for details see the ESI<sup>†</sup>). As previously demonstrated,<sup>11</sup> oligomers of silver ions with organic ligands and anions can be detected in solution by means of ES MS. Although this technique is not illustrative of

the distribution of species in solution, as it can only detect charged species in the gas phase, it does provide interesting information on the self-assembly process before crystallization.

Crystals of **3** crystallize in the cubic space group  $I\bar{4}3d$  with the unit cell parameters of 20.2313(6) Å. Based on single crystal X-ray analysis, TPymT coordinates to three  $\text{Ag}^{\text{I}}$  ions acting as a tris-tripyridine ligand. Each  $\text{Ag}^{\text{I}}$  ion has a distorted hexacoordinate environment formed by the coordination pockets of two neighbouring TPymT ligands (Fig. 2). The average  $\text{Ag}-\text{N}(\text{triazine})$  bond distance is 2.30 Å, while the  $\text{Ag}-\text{N}(\text{pyrimidine})$  bond lengths are 2.51 and 2.58 Å, which are significantly elongated with respect to the  $\text{Ag}-\text{N}(\text{triazine})$  bond. Within the planar trinuclear unit, the  $\text{Ag}^{\text{I}} \cdots \text{Ag}^{\text{I}}$  distance is 6.20 Å, which is 0.24–0.29 Å shorter than those found in the discrete trinuclear analogue  $[\text{Ag}_3(\text{TPymT})(\text{H}_2\text{O})(\text{NO}_3)_3] \cdot \text{H}_2\text{O}$  (**4**).<sup>12</sup> Furthermore, each of the trinuclear  $[\text{Ag}_3\text{TPymT}]^{3+}$  fragments is twisted by  $\sim 70^\circ$  relative to one another imposed by the distorted octahedral  $\text{Ag}^{\text{I}}$  coordination environment.

Similar to complexes **1** and **2**, the formation of the interpenetrating 3D network of **3** is driven by anion- $\pi$ -system interactions, as evidenced by the contacts between  $\text{ClO}_4^-$  with the neighbouring electron deficient *s*-triazine core of TPymT. The  $\text{ClO}_4^-$  anions in **3** are situated directly above the central triazine rings (Fig. 3) with distances between the oxygen atoms of  $\text{ClO}_4^-$  and the centroids of the triazine rings being 3.21 and 3.87 Å.<sup>13</sup> Through these interactions, a 1D chain of alternating anion- $\pi$ -system moieties are formed, thus stabilizing the network.

Since each TPymT coordinates to three  $\text{Ag}^{\text{I}}$  ions and each  $\text{Ag}^{\text{I}}$  ion coordinates to two TPymT ligands, this leads to a complex 2-fold interpenetrating 3D coordination network (Fig. 4). This network can be described as a (10,3)-*a* topology, with each TPymT ligand as a three-connected node and each  $\text{Ag}^{\text{I}}$  cation as a linker. The same topology was also observed in the  $\text{ZnSiF}_6$  complex of 2,4,6-tri(4-pyridyl)-1,3,5-triazine and the  $\text{AgClO}_4$  complex of 1,4,5,8,9,12-hexaazatriphenylene.<sup>14</sup> A comparison of the structures **3** and **4** establishes the vital templating role of the  $\text{ClO}_4^-$  anion vs.  $\text{NO}_3^-$ . The former serves as a driving force in the formation of the

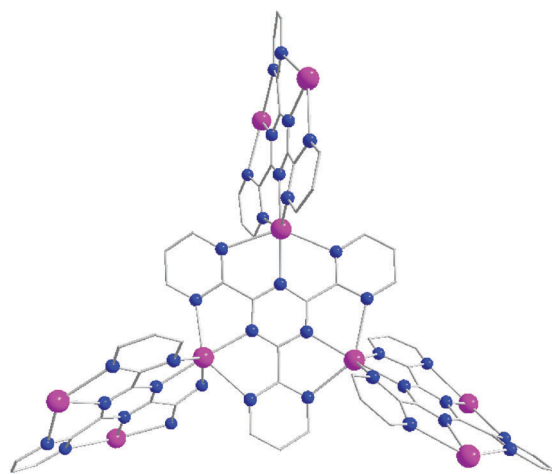


Fig. 2 Ball and stick molecular structure of the  $[\text{Ag}_3\text{TPymT}_4]^{9+}$  segment in the structure of **3** (hydrogen atoms and  $\text{ClO}_4^-$  anions were omitted for clarity). Color code: C = grey, N = blue, Ag = magenta.

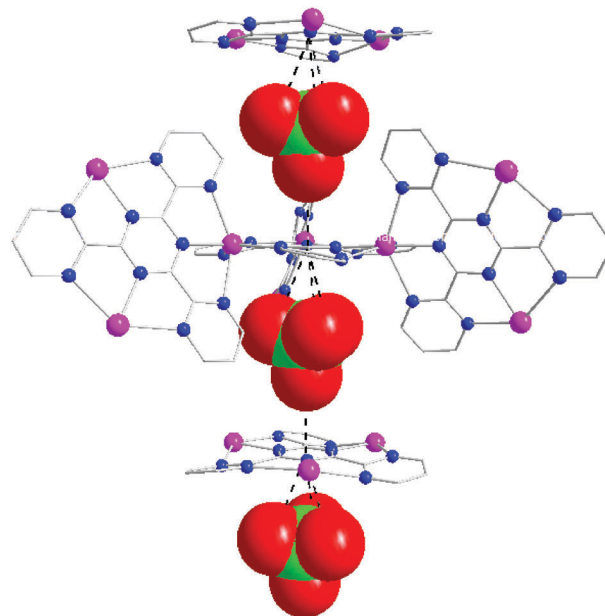


Fig. 3 Ball and stick and spacefill representation of 1D supramolecular pillars constructed through the  $\text{ClO}_4^-$ - $\pi$ -system interactions in the structure of **3** (hydrogen atoms were omitted for clarity). Color code: C = black, Cl = light green, N = blue, Ag = magenta, O = red.

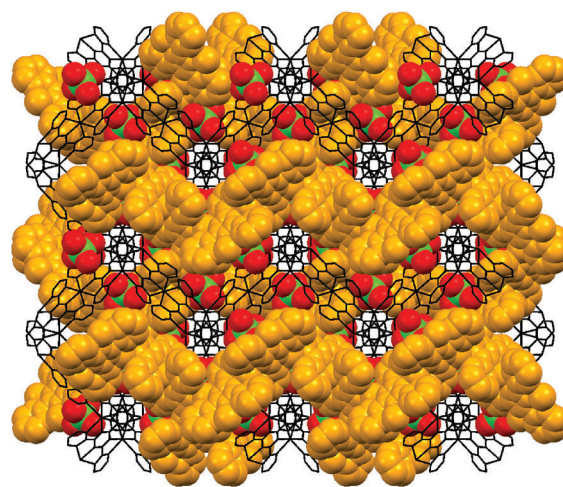


Fig. 4 Spacefill and stick 3D 2-fold interpenetrating supramolecular coordination network of **3** (hydrogen atoms were omitted for clarity). Color code: coordination networks = black and orange, Cl = pale green, O = red.

2-fold interpenetrating 3D coordination network, while the latter yields a discrete trinuclear molecule.<sup>12</sup>

The bulk sample of **3** was studied by means of powder X-ray diffraction (Fig. S6 in the ESI†). The experimental X-ray powder pattern is in agreement with the calculated powder pattern obtained from a single crystal X-ray structure. On the other hand, powder X-ray diffraction analysis of complexes **1** and **2** shows some discrepancies between the predicted and experimental patterns due to extensive evaporation of solvent molecules from the isolated crystals (Fig. S7 and S8 in the ESI†). Nonetheless, several single crystals of each **1** and **2** were analysed *via* single crystal XRD and found to be isostructural.

In summary, 1D, 2D and 3D supramolecular coordination networks were successfully isolated through the use of anion– $\pi$ -system interactions. The  $\pi$ -acidic aromatic moieties in the ligands BPymTz and TPymT provide an ideal platform to induce such interactions. This, coupled with the multiple coordination sites in the ligands, promotes multidimensional growth. In particular, the selective use of  $\text{PF}_6^-$  and  $\text{OTf}^-$  leads to the formation of a 1D ribbon-like chain (1) and a 2D honeycomb-like layered structure (2), respectively, through coordination of BPymTz with  $\text{Ag}^+$ . Furthermore, exploiting such interactions between a rationally designed ligand with three-fold symmetry (TPymT) and  $\text{ClO}_4^-$  enables the formation of a two-fold interpenetrating compact 3D coordination network (3). These three examples provide clear evidence of the pivotal role played by different anions (size and shape) and their interactions with the ligand, which directs the superstructure formation. This strategy offers a unique approach in the development of novel supramolecular assemblies through the use of counter anions as strategic synthons.

This work was financially supported by the NSERC-DG, CFI, ORF, and ERA. We acknowledge the FSR (UCL) for the incoming postdoctoral fellowship co-funded by the Marie Curie actions of the European Commission granted to N. A. Tumanov. We thank SNBL at the ESRF for the beamtime allocation. R. J. Holmberg is also kindly acknowledged for the STM and X-ray powder pattern measurements.

## Notes and references

- (a) H.-J. Schneider, *Angew. Chem., Int. Ed.*, 1991, **30**, 1417; (b) P. Gamez, T. J. Mooibroek, S. J. Teat and J. Reedijk, *Acc. Chem. Res.*, 2007, **40**, 435; (c) B. L. Schottel, H. T. Chifotides and K. R. Dunbar, *Chem. Soc. Rev.*, 2008, **37**, 68; (d) C. Caltagirone and P. A. Gale, *Chem. Soc. Rev.*, 2009, **38**, 520; (e) A. Robertazzi, F. Krull, E.-W. Knapp and P. Gamez, *CrystEngComm*, 2011, **13**, 3293; (f) C. Estarellas, A. Frontera, D. Quiñero and P. M. Deyà, *Angew. Chem., Int. Ed.*, 2011, **50**, 415; (g) A. Frontera, P. Gamez, M. Mascal, T. J. Mooibroek and J. Reedijk, *Angew. Chem., Int. Ed.*, 2011, **50**, 9564; (h) H. T. Chifotides and K. R. Dunbar, *Acc. Chem. Res.*, 2012, **46**, 894; (i) I. V. Krieger, J. S. Freundlich, V. B. Gawandi, J. B. Roberts, V. B. Gawandi, Q. Sun, J. L. Owen, M. T. Fraile, S. I. Huss, J.-L. Lavandera, T. R. Loerger and J. C. Sacchetti, *Chem. Biol.*, 2012, **19**, 1556; (j) K. Bowman-James, A. Bianchi and E. García-España, *Anion Coordination Chemistry*, Wiley-VCH, 2012.
- (a) M. Mascal, A. Armstrong and M. D. Bartberger, *J. Am. Chem. Soc.*, 2002, **124**, 6274; (b) I. Alkorta, I. Rozas and J. Elguero, *J. Am. Chem. Soc.*, 2002, **124**, 8593; (c) D. Quiñero, C. Garau, C. Rotger, A. Frontera, P. Ballester, A. Costa and P. M. Deyà, *Angew. Chem., Int. Ed.*, 2002, **41**, 3389.
- (a) R. Hasenknopf, J.-M. Lehn, B. O. Kneisel, G. Baum and D. Fenske, *Angew. Chem., Int. Ed.*, 1996, **35**, 1838; (b) R. Hasenknopf, J.-M. Lehn, N. Boumediene, A. Dupont-Gervais, A. Van Dorsselaer, B. Kneisel and D. Fenske, *J. Am. Chem. Soc.*, 1997, **119**, 10956; (c) P. D. Beer and P. A. Gale, *Angew. Chem., Int. Ed.*, 2001, **40**, 486; (d) M. J. Hannon, C. L. Painting, E. A. Plummer, L. J. Childs and N. W. Alcock, *Chem. – Eur. J.*, 2002, **8**, 2225; (e) R. Vilar, *Angew. Chem., Int. Ed.*, 2003, **42**, 1460; (f) C. S. Campos-Fernández, B. L. Schottel, H. T. Chifotides, J. K. Bera, J. Bacsa, J. M. Koomen, D. H. Russell and K. R. Dunbar, *J. Am. Chem. Soc.*, 2005, **127**, 12909; (g) M. Shatruk, A. Chouai and K. R. Dunbar, *Dalton Trans.*, 2006, 2184; (h) B. L. Schottel, H. T. Chifotides, M. Shatruk, A. Chouai, L. M. Pérez, J. Bacsa and K. R. Dunbar, *J. Am. Chem. Soc.*, 2006, **128**, 5895.
- (a) X.-P. Zhou, D. Li, T. Wu and X. Zhang, *Dalton Trans.*, 2006, 2435; (b) X.-P. Zhou, D. Li, T. Wu and X. Zhang, *Inorg. Chem.*, 2006, **45**, 7119.
- I. D. Giles, H. T. Chifotides, M. Shatruk and K. R. Dunbar, *Chem. Commun.*, 2011, **47**, 12604.
- W. Kaim and J. Fees, *Z. Naturforsch.*, 1995, **50b**, 123.
- F. H. Case and E. Koft, *J. Am. Chem. Soc.*, 1959, **81**, 905.
- (a) S. Demeshko, S. Dechert and F. Meyer, *J. Am. Chem. Soc.*, 2004, **126**, 4508; (b) P. de Hoog, P. Gamez, I. Mutikainen, U. Turpeinen and J. Reedijk, *Angew. Chem., Int. Ed.*, 2004, **43**, 5815.
- D. A. Safin, Y. Xu, I. Korobkov, D. L. Bryce and M. Murugesu, *CrystEngComm*, 2013, **15**, 10419.
- (a) B. L. Schottel, J. Bacsa and K. R. Dunbar, *Chem. Commun.*, 2005, 46; (b) K. Chainok, S. M. Neville, C. M. Forsyth, W. J. Gee, K. S. Murray and S. R. Batten, *CrystEngComm*, 2012, **14**, 3717.
- (a) A. M. Bond, R. Colton, Y. A. Mah and J. C. Traeger, *Inorg. Chem., J. Chem. Soc., Chem. Commun.*, 1995, 1679; (c) E. C. Constable, C. E. Housecroft, B. M. Kariuki, N. Kelly and C. B. Smith, *Inorg. Chem. Commun.*, 2002, **5**, 199; (d) F. Bachechi, A. Burini, R. Galassi, B. R. Pietroni and M. Ricciutelli, *Inorg. Chim. Acta*, 2004, **357**, 4349.
- D. A. Safin, A. Pialat, I. Korobkov and M. Murugesu, *Chem. – Eur. J.*, 2015, **21**, 6144.
- P. U. Maheswari, B. Modec, A. Pevec, B. Kozlevcar, C. Massera, P. Gamez and J. Reedijk, *Inorg. Chem.*, 2006, **45**, 6637.
- (a) B. F. Abrahams, S. R. Batten, H. Hamit, B. F. Hoskins and R. Robson, *Chem. Commun.*, 1996, 1313; (b) B. F. Abrahams, P. A. Jackson and R. Robson, *Angew. Chem., Int. Ed.*, 1998, **37**, 2656.